occurs with the changes in specimen thickness and defocus (Hirabayashi, Hiraga & Shindo 1981; Hiraga *et al.*, 1981). The image of Fig. 7 shows intergrowth of the Au_4Mn, $Au_{22}Mn_6$ and $Au_{31}Mn_9$ structures, where the respective unit cells are outlined. The appearance of the $Au_{31}Mn_9$ structure is not surprising, because this structure is formed when the Au–20·7 at.% Mn alloy is annealed at 673 K as reported in part I. It is noted that the $Au_{31}Mn_9$ structure exists at intersections of the three-dot columns aligned parallel to the two orthogonal directions [210] and [1$\bar{2}$0]. This is reasonably understood because the $Au_{31}Mn_9$ structure is composed of square-shaped islands of the Au_4Mn structure and the islands are separated by 2*d*-APB along the two orthogonal directions as described in part I.

The image of Fig. 8 shows a random appearance of butterfly-shaped spots in the surrounding area of Fig. 7. These spots began to appear after electron irradiation for several hundred seconds, and grew with the irradiation time. The Mn-atom rows cannot be recognized in the dark spots, but are clearly seen along the middle lines between the paired spots. These lines are the so-called 'line of no contrast' in the image of the dislocation loops. The line of no contrast lies along the direction [110] or [$\bar{1}$10] as indicated by arrows. This is also the case in Fig. 5. The dark spots are ascribed to strain field around dislocation loops lying on {111} planes, of which the diameter is estimated as 10–30 Å. Similar dark spots have been observed in the previous study (Hirabayashi, 1980; Terasaki *et al.*, 1981).

We are grateful to Mr H. Ota and Mr E. Aoyagi for their help in the HVHREM work. The present work has partly been supported by a Grant-in-Aid for Scientific Research from the Ministry of Education, Science and Culture.

References

AMELINCKX, S. (1978–79). *Chem. Scr.* **14**, 197–206.

HIRABAYASHI, M. (1980). *Electron Microscopy*–1980, Vol. 4 (*Proceedings of the 6th International Conference on High-Voltage Electron Microscopy, Antwerp*), edited by P. BREDEROO & J. VAN LANDUYT, pp. 142–149. Leiden: Seventh European Congress on Electron Microscopy Foundation.

HIRABAYASHI, M., HIRAGA, K. & SHINDO, D. (1981). *J. Appl. Cryst.* **14**, 169–177.

HIRABAYASHI, M., HIRAGA, K., SHINDO, D. & YAMAMOTO, T. (1981). *Sci. Rep. Res. Inst. Tohoku Univ. Ser. A*, **29**, Suppl. 1, 1–6.

HIRAGA, K., SHINDO, D. & HIRABAYASHI, M. (1980). *Electron Microscopy*–1980, Vol. 4 (*Proceedings of the 6th International Conference on High-Voltage Electron Microscopy, Antwerp*), edited by P. BREDEROO & J. VAN LANDUYT, pp. 170–173. Leiden: Seventh European Congress on Electron Microscopy Foundation.

HIRAGA, K., SHINDO, D. & HIRABAYASHI, M. (1981). *J. Appl. Cryst.* **14**, 185–190.

HIRAGA, K., SHINDO, D., HIRABAYASHI, M., TERASAKI, O. & WATANABE, D. (1980). *Acta Cryst.* B**36**, 2550–2554.

TERASAKI, O., WATANABE, D., HIRAGA, K., SHINDO, D. & HIRABAYASHI, M. (1980). *Micron*, **11**, 235–240.

TERASAKI, O., WATANABE, D., HIRAGA, K., SHINDO, D. & HIRABAYASHI, M. (1981). *J. Appl. Cryst.* **14**, 392–400.

VAN TENDELOO, G. (1980). *J. Microsc. (Oxford)*, **119**, 125–140.

WATANABE, D. (1957). *Acta Cryst.* **10**, 483–485.

WATANABE, D. (1979). *Modulated Structures*–1979, *AIP Conf. Proc.* No. 53, edited by J. M. COWLEY, J. B. COHEN, M. B. SALAMON & B. J. WUENSCH, pp. 229–239. New York: American Institute of Physics.

Acta Cryst. (1982). A**38**, 274–285

Symmetrized Multipole Analysis of Coupled Orientation–Translation Distributions

BY MIKKO KARA

Department of Physics, University of Helsinki, Siltavuorenpenger 20 *D, SF*-00170 *Helsinki* 17, *Finland*

(*Received* 28 *May* 1981; *accepted* 26 *October* 1981)

Abstract

Symmetrized multipole formalism, in diffraction studies of orientationally disordered molecular crystals, is generalized to include coupling between orientations and translations of a rigid body and anharmonicity in the center-of-mass motion. This generalized formalism is intended for use with direct multipole analysis of the observed form factors. In the relationships between the radial multipole coefficients of the dynamic and static density, correlations cause a mixing in the multipole order. In the dynamic form factor the parameters describing the coupling are linear combinations of the multipole expansion coefficients of the corresponding rigid-body distribution. Parameters describing anisotropy are directly the multipole expansion coefficients

0567-7394/82/020274-12$01.00

of the rigid-body center-of-mass distribution. As an example of the formalism, neutron diffraction data from cubic KCN, NaCN, KOD, NaOD and CBr_4 and rhombohedral $RbNO_3$ are reanalyzed with direct multipole analysis. In these examples the importance of coupling seems to grow with the complexity of the crystal.

1. Introduction

In diffraction studies of orientationally disordered molecular crystals it is often assumed as a first approximation that the molecule behaves as a rigid body and that there are no correlations between the orientational and translational motion.

If infrared and Raman spectroscopic data are available, one can estimate the contribution from the internal modes and the validity of the first approximation (*cf.* Willis & Pryor, 1975, Ch. 6). For small atomic displacements the orientation–translation coupling is described with the **TLS** matrix formalism of Schomaker & Trueblood (1968). The **S** matrix takes into account correlations in the quadratic approximation, and is therefore zero when the site symmetry is $\bar{1}$. In general **S** is an asymmetric matrix with eight independent elements.

In orientationally disordered molecular crystals the molecules are often undergoing hindered rotation. Consequently, the atoms do not have well-defined equilibrium positions with respect to which the matrices **T**, **L** and **S** could be calculated. Because of this large libration amplitude orientation–translation coupling might be of importance in these materials. For higher symmetries with large molecules, such as cubic CBr_4, coupling could be a consequence of the steric hindrance. In more complex symmetries, such as rhombohedral $RbNO_3$, coupling is already evident from geometrical reasons.

In these crystals the pure orientational problem is appreciated with the symmetrized multipole formalism (Kara & Kurki-Suonio, 1981, hereafter referred to as I). In this formalism the experimental information is parametrized with the multipole expansion coefficients of the orientational probability density function of the molecule. These coefficients determine also the libration matrices, which transform the static radial densities into dynamic ones. This connection makes the formalism useful for direct multipole analysis and for combined charge and nuclear density studies.

It is also possible to include in the multipole method the effect of internal vibrations, independent of the external motion (Kurki-Suonio, Merisalo, Vahvaselkä & Larsen, 1976).

The multipole method has been generalized to include orientation–translation coupling for cubic sites by Press, Grimm & Hüller (1979).

This paper aims towards a generalization from distribution function $f(\omega)$ for $f(\omega,\mathbf{R})$ using multipole representations. It includes orientation–translation coupling and center-of-mass anharmonicity for all body and site symmetries. The influence of this generalization on the relationship between the static and dynamic radial densities is studied for various approximations. This formalism is then applied, together with the direct multipole analysis, for several examples typical among orientationally disordered molecular crystals.

The predecessor and basic reference for this work is I, from which symbols and procedures are here largely adopted.

2. Probability distribution of rigid-body motions

The dynamic molecular form factor $F(\mathbf{S})$, obtained from coherent elastic scattering experiments, is the Fourier transform of the dynamic density $\rho_{TR}(\mathbf{r})$,

$$F(\mathbf{S}) = \int \exp(2\pi \mathbf{S}.\mathbf{r})\, \rho_{TR}(\mathbf{r})\, \mathrm{d}\mathbf{r}, \qquad (1)$$

where **S** is the scattering vector for Bragg diffraction. In the rigid-body approximation, the dynamic density and the static density $\sigma(\mathbf{r})$ are related by the probability distribution $f(\omega,\mathbf{R})$,

$$\rho_{TR}(\mathbf{r}) = \iint f(\omega,\mathbf{R})\, \hat{R}(\omega)\, \hat{T}(\mathbf{R})\, \sigma(\mathbf{r})\, \mathrm{d}\omega\, \mathrm{d}\mathbf{R}, \qquad (2)$$

where $\hat{R}(\omega)$ denotes rotation about the center of mass through the Euler angles $\omega = \alpha, \beta, \gamma$ and $\hat{T}(\mathbf{R})$ denotes the translation of the center of mass of the rigid body. Here these two operations commute.

The static density $\sigma(\mathbf{r})$ describes the molecule at rest, when the dynamic density is the corresponding observed time-averaged distribution of the body in motion. Rigid-body approximation means that the internal motion does not contribute to $\rho_{TR}(\mathbf{r})$ or that it gives a separable contribution.

The integrations in (2) are over all rotations and translations, *i.e.*

$$\iint \mathrm{d}\omega\, \mathrm{d}\mathbf{R} = \int_0^{2\pi}\int_0^{\pi}\int_0^{2\pi} \mathrm{d}\alpha \sin\beta\, \mathrm{d}\beta\, \mathrm{d}\gamma \times \int_0^{\infty}\int_0^{\pi}\int_0^{2\pi} R^2\, \mathrm{d}R \sin\theta\, \mathrm{d}\theta\, \mathrm{d}\varphi.$$

$f(\omega,\mathbf{R})$ is the probability distribution of rotational and translational displacements of the molecule, hence it is non-negative $f \geq 0$ and normalized $\iint f(\omega,\mathbf{R})\, \mathrm{d}\omega\, \mathrm{d}\mathbf{R} = 1$. Furthermore, the site symmetry imposes certain limitations on its nature. They can be defined generally by the statement $f(\omega,\mathbf{R})$ is site symmetric if for any static density $\sigma(\mathbf{r})$ the corresponding dynamic density $\rho_{TR}(\mathbf{r})$ is site symmetric (*cf.* I).

When the rotational and translational degrees of freedom are *independent* $f(\omega,\mathbf{R})$ is

$$f(\omega,\mathbf{R}) = f(\omega)\, \tau(\mathbf{R}). \qquad (3)$$

In this case the dynamic density becomes

$$\rho_{TR}(\mathbf{r}) = \int \tau(\mathbf{R})\, \hat{T}(\mathbf{R})\, \rho_R(\mathbf{r})\, \mathrm{d}\mathbf{R} = \int \tau(\mathbf{R})\, \rho_R(\mathbf{r}')\, \mathrm{d}\mathbf{R}, \quad (4)$$

where $\mathbf{r}' = \mathbf{r} - \mathbf{R}$ and the rotational dynamic density $\rho_R(\mathbf{r})$ is

$$\rho_R(\mathbf{r}) = \int f(\omega)\, \hat{R}(\omega)\, \sigma(\mathbf{r})\, \mathrm{d}\omega. \quad (5)$$

$f(\omega)$ and $\tau(\mathbf{R})$ are the orientational and translational probability distributions of the molecule, respectively. In general these two distributions are

$$\mathbf{f}(\omega) = \int f(\omega,\mathbf{R})\, \mathrm{d}\mathbf{R} \quad (6a)$$

$$\boldsymbol{\tau}(\mathbf{R}) = \int f(\omega,\mathbf{R})\, \mathrm{d}\omega. \quad (6b)$$

The *uncorrelated approximation* is now defined as

$$f_0(\omega,\mathbf{R}) = \mathbf{f}(\omega).\boldsymbol{\tau}(\mathbf{R}). \quad (7)$$

We can also quite generally express $f(\omega,\mathbf{R})$ in either of the two forms

$$f(\omega,\mathbf{R}) = \mathbf{f}(\omega)\, \tau^c(\mathbf{R}|\omega), \quad (8a)$$

$$f(\omega,\mathbf{R}) = \boldsymbol{\tau}(\mathbf{R})\, f^c(\omega|\mathbf{R}), \quad (8b)$$

where $\tau^c(\mathbf{R}|\omega)$ is the conditional probability for the center of mass to be at $\mathbf{R}$, if the orientation of the molecule is ω.

$f^c(\omega|\mathbf{R})$ is the conditional probability for finding the molecule in orientation ω, if its center of mass is displaced to $\mathbf{R}$. The conditional probability $f^c(\omega|\mathbf{R})$ defines the rotational dynamic density

$$\rho_R(\mathbf{r};\mathbf{R}) = \int f^c(\omega|\mathbf{R})\, \hat{R}(\omega)\, \sigma(\mathbf{r})\, \mathrm{d}\omega, \quad (9)$$

where the center-of-mass position $\mathbf{R}$ occurs as a parameter. The final dynamic density is now

$$\rho_{TR}(\mathbf{r}) = \int \boldsymbol{\tau}(\mathbf{R})\, \hat{T}(\mathbf{R})\, \rho_R(\mathbf{r};\mathbf{R})\, \mathrm{d}\mathbf{R} = \int \boldsymbol{\tau}(\mathbf{R})\, \rho_R(\mathbf{r}';\mathbf{R})\, \mathrm{d}\mathbf{R}. \quad (10)$$

Correspondingly $\tau^c(\mathbf{R}|\omega)$ defines the translational dynamic density

$$\rho_T(\mathbf{r};\omega) = \int \tau^c(\mathbf{R}|\omega)\, \hat{T}(\mathbf{R})\, \sigma(\mathbf{r})\, \mathrm{d}\mathbf{R} = \int \tau^c(\mathbf{R}|\omega)\, \sigma(\mathbf{r}')\, \mathrm{d}\mathbf{R}, \quad (11)$$

where the Euler angles ω of the orientation of the molecule are parameters. The final dynamic density is then

$$\rho_{TR}(\mathbf{r}) = \int \mathbf{f}(\omega)\, \hat{R}(\omega)\, \rho_T(\mathbf{r};\omega)\, \mathrm{d}\omega. \quad (12)$$

Representations (8)–(12) are not practically very useful. They are given here only to relate the treatment to the earlier work I. In the above equations $f(\omega,\mathbf{R})$ and $\rho_{TR}(\mathbf{r})$ are necessarily always site symmetric. From the definition of the site symmetry of $f(\omega,\mathbf{R})$ it follows (this is proved later) that $\boldsymbol{\tau}(\mathbf{R})$ and $\mathbf{f}(\omega)$ are site symmetric. In the uncorrelated approximation (7) $\mathbf{f}(\omega)$ and $\boldsymbol{\tau}(\mathbf{R})$ are, of course, always site symmetric. $f^c(\omega|\mathbf{R})$, $\rho_R(\mathbf{r};\mathbf{R})$, $\tau^c(\mathbf{R}|\omega)$ and $\rho_T(\mathbf{r};\omega)$ are lower than site symmetric, since they are defined at an arbitrary center-of-mass position and orientation of the molecule.

3. The multipole formalism

(A) *Representation for the orientational distribution*

In I we introduced the basis $\{C^l_{nrmp}(\omega)\}$ for the representation of the orientational distribution

$$f(\omega) = \sum_{lnrmp} a^l_{nrmp}\, C^l_{nrmp}(\omega). \quad (13)$$

The first term $a^0_{0+0+} = 1/8\pi^2$ corresponds to free rotations. These real rotator functions have the normalization

$$\int \{C^l_{nrmp}(\omega)\}^2\, \mathrm{d}\omega = 8\pi^2/2l + 1. \quad (14)$$

They define the transformation properties of the normalized real spherical harmonics under rotation.

In this basis, in the case of independent rotations and translations and for the uncorrelated approximation, the body and site symmetry are easily taken into consideration. When the static density and the rotational dynamic density are represented by the multipole expansions,

$$\sigma(\mathbf{r}) = \sum_{lmp} \sigma_{lmp}(r)\, y_{lmp}(\theta,\varphi) \quad (15)$$

$$\rho_R(\mathbf{r}) = \sum_{lnr} \rho^R_{lnr}(r)\, y_{lnr}(\theta,\varphi) \quad (16)$$

and substituted in (5), their radial terms are related by the libration matrices $\mathsf{B}_l = [(8\pi^2/2l + 1)\, a^l_{nrmp}]$,

$$\boldsymbol{\rho}^R_l(\mathrm{r}) = \mathsf{B}_l\, \boldsymbol{\sigma}_l(r). \quad (17)$$

The index rules for the indices *lmp*, for the body-symmetric static density, and for the indices *lnr*, for the site-symmetric dynamic rotational density, apply also to the body- and site-symmetric orientational distribution.

In the presence of orientation–translation correlations, the conditional distribution $f^c(\omega|\mathbf{R})$ enters with the multipole representation

$$f^c(\omega|\mathbf{R}) = \sum_{lnrmp} a^l_{nrmp}(\mathbf{R}) C^l_{nrmp}(\omega). \quad (18)$$

The radial terms of the static density are now related, through (9), to the radial terms of the rotational dynamic density $\rho_R(\mathbf{r};\mathbf{R})$ by position-dependent libration matrices $\mathsf{B}_l(\mathbf{R}) = [(8\pi^2/2l + 1)\, a^l_{nrmp}(\mathbf{R})]$,

$$\boldsymbol{\rho}^R_l(r;\mathbf{R}) = \mathsf{B}_l(\mathbf{R})\, \boldsymbol{\sigma}_l(r). \quad (19)$$

At this stage these position-dependent libration matrices contain more elements than the constant matrices $\mathsf{B}_l = \mathsf{B}_l\ (\mathbf{R} = 0)$ in (17), because $\rho_R(\mathbf{r};\mathbf{R})$ is lower than site symmetric. But, since $\boldsymbol{\tau}(\mathbf{R})$ is site symmetric $f^c(\omega|\mathbf{R})$ is site symmetrized in the convolution integral (10).

All the above results are also valid for cubic site symmetry and for cubic and icosahedral body symmetries, when the corresponding rotators are employed (*cf.* I).

(*B*) *Representation for the translational distribution*

Small translational anisotropy can be adequately described using the real spherical harmonics as a basis for the representation of $\tau(\mathbf{R})$,

$$\tau(\mathbf{R}) = \sum_{tuv} \tau_{tuv}(R) y_{tuv}(\theta_R,\varphi_R). \tag{20}$$

These spherical harmonics have the normalization

$$\int_0^{\pi}\int_0^{2\pi} y_{tuv}(\theta,\varphi)^2 \sin\theta \,\mathrm{d}\theta\,\mathrm{d}\varphi = 1. \tag{21}$$

Normalization of the translational distribution itself imposes the following condition on the radial terms

$$\sqrt{4\pi}\int_0^{\infty} R^2\, \tau_{00+}(R)\,\mathrm{d}R = 1. \tag{22}$$

Whatever radial basis is used for the representation of $\tau_{tuv}(R)$, the site symmetry of $\tau(\mathbf{R})$ is defined by selection rules of the indices *tuv* (Kurki-Suonio, Merisalo & Peltonen, 1979). In cubic site symmetries the y_{tuv} combine to form the cubic harmonics $K_{t'u'}$.

For strongly anharmonic translations representation (20) is not very useful, since then too many parameters are needed.

(*C*) *Representation for the orientational–translational distribution*

The above two bases can be combined to give a product basis for the representation of $f(\omega,\mathbf{R})$:

$$f(\omega,\mathbf{R}) = \sum_{tuv}\sum_{lnrmp} {}_{uv}^{t}A^{l}_{nrmp}(R) y_{tuv}(\theta_R,\varphi_R)\, C^{l}_{nrmp}(\omega). \tag{23}$$

In this formalism this basis will lead to more simple symmetry arguments concerning the total distribution than any other combination; *i.e.* with this choice we get to the structure-factor product of two real spherical harmonics, which is easy to symmetrize. The expansion coefficients fulfil the normalization condition

$$8\pi^2\sqrt{4\pi}\int_0^{\infty} R^2\, {}_{0+}^{0}A^{0}_{0+0+}(R)\,\mathrm{d}R = 1. \tag{24}$$

If rotations and translations are independent, we have

$${}_{uv}^{t}A^{l}_{nrmp}(R) = a^{l}_{nrmp}\, \tau_{tuv}(R). \tag{25}$$

The generalized rotational and translational distributions are, according to their definitions (6),

$$\mathbf{f}(\omega) = \sum_{lnrmp}\left\{\sqrt{4\pi}\int_0^{\infty} R^2\, {}_{0+}^{0}A^{l}_{nrmp}(R)\,\mathrm{d}R\right\} C^{l}_{nrmp}(\omega) \tag{26}$$

$$\tau(\mathbf{R}) = \sum_{tuv}\{8\pi^2\, {}_{uv}^{t}A^{0}_{0+0+}(R)\} y_{tuv}(\theta_R,\varphi_R). \tag{27}$$

Thus multipole expansion coefficients of the uncorrelated approximation $f_0(\omega,\mathbf{R})$ are

$${}_{uv}^{t}B^{l}_{nrmp}(R) = 8\pi^2\sqrt{4\pi}\, {}_{uv}^{t}A^{0}_{0+0+}(R)\int_0^{\infty} R^2\, {}_{0+}^{0}A^{l}_{nrmp}(R)\,\mathrm{d}R. \tag{28}$$

For angle-independent distribution these are equal to the original expansion coefficients

$${}_{uv}^{t}B^{0}_{0+0+}(R) = {}_{uv}^{t}A^{0}_{0+0+}(R), \tag{29}$$

and there are therefore no correlations; this is trivial. If for anisotropic or isotropic vibrations the expansion coefficients all fulfil the condition

$${}_{uv}^{t}A^{l}_{nrmp}(R) = a^{l}_{nrmp}\, {}_{uv}^{t}A^{0}_{0+0+}(R), \tag{30}$$

rotations and translations are again uncorrelated,

$${}_{uv}^{t}B^{l}_{nrmp}(R) = {}_{uv}^{t}A^{l}_{nrmp}(R). \tag{31}$$

Those expansion coefficients ${}_{uv}^{t}A^{l}_{nrmp}(R)$ of $f(\omega,\mathbf{R})$ which do not fulfil the condition (30) describe rotation–translation correlations. In particular, for spherical vibrations there can also be correlations if ${}_{0+}^{0}A^{l}_{nrmp}(R)$ do not fulfil (30).

It should be noted that indices *tuv* and *lnr* in $f_0(\omega,\mathbf{R})$ are determined, separately, by the site symmetry, since both $\tau(\mathbf{R})$ and $\mathbf{f}(\omega)$ are site symmetric. For these expansion coefficients condition (30) is natural since it then becomes equal to (25).

4. The structure factor

Because this formalism is mainly intended for use with the direct multipole analysis (Ahtee, Kurki-Suonio, Lucas & Hewat, 1979) of the observed form factors, we shall next study the relationship between the multipole expansions for the static density and the final dyamic density in reciprocal space. There we have schematically

$$F(\mathbf{S})\left\{\begin{array}{lll}
\tau(\mathbf{R}) & \mathbf{f}(\omega)\text{ or }\mathsf{B}_l & \\
\longleftrightarrow & f_0(\mathbf{S}) \longleftrightarrow & (32a)\\
 & f(\omega,\mathbf{R}) & \\
\longleftrightarrow & & (32b)\\
\mathbf{f}(\omega) & \tau^c(\mathbf{R}|\omega) & \\
\longleftrightarrow & \mathbf{T}(\mathbf{S};\omega) \longleftrightarrow & (32c)\\
\tau(\mathbf{R}) & f^c(\omega|\mathbf{R})\text{ or }\mathsf{B}_l(\mathbf{R}) & \\
\longleftrightarrow & f(\mathbf{S};\mathbf{R}) \longleftrightarrow & (32d)
\end{array}\right\} g(\mathbf{S}).$$

These equations illustrate how, for the different rigid-body distributions introduced in § 2, the static form factor $g(\mathbf{S})$ relates to the final dynamic form factor $F(\mathbf{S})$. $F(\mathbf{S})$ and $g(\mathbf{S})$ are Fourier transforms of the final dynamic density $\rho_{TR}(\mathbf{r})$ and the static density $\sigma(\mathbf{r})$, respectively. $T(\mathbf{S})$ and $f(\mathbf{S})$ are the temperature factor and rotational form factor, Fourier transforms of the translational dynamic density and rotational dynamic density, respectively. The last two relations (32*c*) and (32*d*) are given to show the meaning of the conditional distributions and that these distributions are not practically very useful.

In multipole formulation of the problem the dynamic molecular form factor in cases (32*a*) and (32*b*) are

$$F_0(\mathbf{S}) = \sum_{tuv} T_{tuv}(S)\, y_{tuv}(\theta_S,\varphi_S) \sum_{lnr} f_{lnr}(S)\, y_{lnr}(\theta_S,\varphi_S) \tag{33a}$$

$$F(\mathbf{S}) = \sum_{tuv} \sum_{lnr} {}_{tuv}F_{lnr}(S)\, y_{tuv}(\theta_S,\varphi_S)\, y_{lnr}(\theta_S,\varphi_S). \tag{33b}$$

The radial terms are the Fourier–Bessel transformations

$$T_{tuv}(S) = 4\pi i^t \int_0^\infty \tau_{tuv}(R)\, j_t(2\pi SR)\, R^2\, \mathrm{d}R \tag{34a}$$

$$f_{lnr}(S) = \sum_{mp} (8\pi^2/2l+1)\, a^l_{nrmp}\, g_{lmp}(S)$$

or $$\mathbf{f}_l(S) = \mathsf{B}_l\, \mathbf{g}_l(S)$$

$${}_{tuv}F_{lnr}(S) = \sum_{mp} (8\pi^2/2l+1)\, 4\pi i^t \times \int_0^\infty {}_{uv}^{t}A^l_{nrmp}(R)\, j_t(2\pi SR)\, R^2\, \mathrm{d}R\, g_{lmp}(S), \tag{34b}$$

where $\mathbf{f}_l$ and $\mathbf{g}_l$ denote vectors and

$$g_{lmp}(S) = 4\pi i^l \int_0^\infty \sigma_{lmp}(r)\, j_l(2\pi rS)\, r^2\, \mathrm{d}r \tag{35}$$

is a radial multipole expansion coefficient of the static form factor $g(\mathbf{S})$:

$$g(\mathbf{S}) = \sum_{lmp} g_{lmp}(S)\, y_{lmp}(\theta_S,\varphi_S). \tag{36}$$

The molecular form factor has the site-symmetric multipole expansion

$$F(\mathbf{S}) = \sum_{lnr} F_{lnr}(S)\, y_{lnr}(\theta_S,\varphi_S). \tag{37}$$

The uncorrelated part of (33*b*) is of the form (33*a*), *i.e.* products of two site-symmetric terms, and therefore necessarily of the site-symmetric form (37). The correlated part of (33*b*), and of $f(\omega,\mathbf{R})$, is site symmetric if the sum over products of two real spherical harmonics weighted with ${}_{tuv}F_{lnr}(S)$ reduces to the site-symmetric form (37). In general, site symmetrization of these terms can be done by using the coupling rule for spherical harmonics together with the index-picking rules given for them in I (*cf.* Rose, 1957, Ch. 10).

The body symmetry of $F(\mathbf{S})$ and $f(\omega,\mathbf{R})$ comes always from the body-symmetric index rules concerning indices *lmp* in the body-symmetric static density.

The site symmetry of $\mathbf{f}(\omega)$ and $\boldsymbol{\tau}(\mathbf{R})$, in general, is proved in the following way: In $F(\mathbf{S})$ terms with different (t,l) values are linearly independent, since they have different radial behavior. From the definition of the site symmetry of $f(\omega,\mathbf{R})$ it follows that $F(\mathbf{S})$ must be site symmetric for arbitrary $g_{lmp}(S)$. This stipulates that each partial sum in (33*b*), with different (t,l) values, must be site symmetric. In particular, it follows that when $t = 0$ or $l = 0$ these partial sums must separately be site symmetric, and therefore $\mathbf{f}$ and $\boldsymbol{\tau}$ are site symmetric.

Solvability of $f(\omega,\mathbf{R})$ by direct multipole analysis

In the presence of correlations the number of parameters in the dynamic form factor is large, and therefore a fit is not a very good method for their solution.

Direct multipole analysis determines each radial term $F_{lnr}(S)$ directly and independently from the observed $F(hkl)$ values (Ahtee *et al.*, 1979), and gives thus a more reliable method for obtaining information about $f(\omega,\mathbf{R})$, especially about its multipole expansion coefficients.

The different possible physical situations are given in *A*, *B*, *C*, *D* below.

A. Angle-independent distribution. Each $F_{lnr}(S)$ gives direct information about the center-of-mass motion of the molecule,

$$F_{lnr}(S) = T_{lnr}(S)\, (1/\sqrt{4\pi})\, g_{00+}(S). \tag{38}$$

B. Isotropic harmonic vibrations uncoupled to rotations. Each observed $F_{lnr}(S)$ is now simply a sum of spherical Bessel functions of the same multipole order l, weighted with the Debye–Waller factor

$$F_{lnr}(S) = \mathrm{DWF}(8\pi^2/2l+1) \sum_{mp} a^l_{nrmp}\, g_{lmp}(S). \tag{39}$$

For high body symmetries the low multipole order coefficients a^l_{nrmp} can be solved, since there is then only one term in the sum (*cf.* I).

C. Anisotropic vibrations uncoupled to rotations. Each $F_{lnr}(S)$ is a sum of $g_{lmp}(S)$ terms of different site-symmetric multipole orders, weighted with the integral (34*a*). If both $\tau(\mathbf{R})$ and $f(\omega)$ converge rapidly,

their multipole expansion coefficients are separable (*cf. Examples*).

D. Orientation–translation correlations. $F_{lnr}(S)$ is a combination of different body-symmetric $g_{lmp}(S)$ terms, weighted with the integral in (34*b*). All body-symmetric $g_{lmp}(S)$ terms can contribute to $F_{l'n'r'}(S)$ at each multipole order l' separately. But naturally most significant are those terms $g_{lmp}(S)$ where $l < l'$. This emphasizes the significance of high molecular symmetry for the convergence of the correlated part of $F(\mathbf{S})$. On the other hand, for each (t,l) value the number of terms in $F(\mathbf{S})$ describing correlations depends on the site symmetry. Therefore, high site symmetry is also important for the convergence of the correlated part of $F(\mathbf{S})$.

The multipole expansion coefficients of $f(\omega,\mathbf{R})$ describing correlations cannot be solved separately. Coupling appears quantitatively only as a correction in the orientational parameters a^l_{nrmp}.

5. Examples

In the following examples the stationary wave functions of an isotropic harmonic oscillator are used as the radial basis for $f(\omega,\mathbf{R})$ and $\tau(\mathbf{R})$ (*cf.* Kurki-Suonio *et al.*, 1979).

Linear ion at cubic m3m site

$M^+(XY)^-$ compounds, where a linear ion is at a cubic $m3m$ site, form an extended group of orientationally disordered molecular crystals. In the rigid-body approximation the static radial form factors become

$$g_{lmp}(S) = 4\pi i^l y_{lmp}(h_0 k_0 l_0) \times \{g_x j_l(2\pi S r_1) + g_y j_l(2\pi S r_2)\}, \quad (40)$$

where $(h_0 k_0 l_0)$ is the at-rest orientation of the XY^- ion, (100) for example, g_x and g_y are the scattering lengths of X and Y atoms, respectively, and r_1 and r_2 are their distances to the center of mass of the ion. $j_l(x)$ are the spherical Bessel functions. For a symmetric linear molecule l would be even because of the inversion symmetry. In the structure factor, terms deriving their origin from the uncorrelated probability distribution are of the form, $b_{xy} = 2\pi\langle u^2_{xy}\rangle^{1/2}$,

$$R_l i^l \exp(-\tfrac{1}{2}b^2_{xy} S^2)\{g_x j_l(2\pi S r_1) + g_y j_l(2\pi S r_2)\} K_{l1}(\theta_S, \varphi_S) \quad (41)$$

up to $l = 10$. For a linear ion the multipole expansion for $f(\omega)$ in terms of cubic site – non-cubic body rotators (*cf.* I) reduces to

$$f(\theta,\varphi) = \sum_l R_l K_{l1}(\theta,\varphi), \quad (42)$$

where $R_0 = 1/\sqrt{4\pi}$. Lowest-order terms deriving their origin from the anharmonic translational probability distribution of the dipole are

$$B_1 \exp(-\tfrac{1}{2}b^2_{xy} S^2)\{\tfrac{15}{8} - \tfrac{5}{2}b^2_{xy} S^2 + \tfrac{1}{2}(b_{xy} S)^4\} \times \{g_x j_0(2\pi S r_1) + g_y j_0(2\pi S r_2)\} K_{01}(\theta_S, \varphi_S), \quad (43a)$$

$$B_2 \exp(-\tfrac{1}{2}b^2_{xy} S^2)(b_{xy} S)^4\{g_x j_0(2\pi S r_1) + g_y j_0(2\pi S r_2)\} \times K_{41}(\theta_S, \varphi_S), \quad (43b)$$

$$B_3 \exp(-\tfrac{1}{2}b^2_{xy} S^2)(b_{xy} S)^6\{g_x j_0(2\pi S r_1) + g_y j_0(2\pi S r_2)\} \times K_{61}(\theta_s, \varphi_S), \quad (43c)$$

where

$$B_1 = \tau_{401}\pi\sqrt{2}(\langle u^2_{xy}\rangle^{1/2})^3,$$

$$B_2 = \tau_{441}\pi\sqrt{2}(\langle u^2_{xy}\rangle^{1/2})^3$$

and

$$B_3 = -\tau_{662}\pi\sqrt{2}(\langle u^2_{xy}\rangle^{1/2})^3.$$

The first two coupling terms come from the products [*cf.* (33b)]

$$\sum_{uvnr} {}_{11uv}A^3_{nr1}\, y_{1uv}(\theta_S,\varphi_S) y_{3nr}(\theta_S,\varphi_S) = \alpha_1 K_{41}(\theta_S,\varphi_S) \quad (44)$$

$$\sum_{uvnr} {}_{11uv}A^7_{nr1} y_{1uv}(\theta_S,\varphi_S)\, y_{7nr}(\theta_S,\varphi_S) = \alpha_2 K_{61}(\theta_S,\varphi_S) + \alpha_3 K_{81}(\theta_S,\varphi_S), \quad (45)$$

where α_1 is a linear combination of the five different coefficients ${}_{11uv}A^3_{nr1}$ and α_2 and α_3 are different linear combinations of the eight possible coefficients ${}_{11uv}A^7_{nr1}$. In the structure factor these coupling terms are

$$RT_1 \exp(-\tfrac{1}{2}b^2_{xy} S^2)(b_{xy} S)\{g_x j_3(2\pi S r_1) + g_y j_3(2\pi S r_2)\} \times K_{41}(\theta_S,\varphi_S), \quad (46)$$

$$\exp(-\tfrac{1}{2}b^2_{xy} S^2)(b_{xy} S)\{g_x j_7(2\pi S r_1) + g_y j_7(2\pi S r_2)\} \times \{RT_2 K_{61}(\theta_S,\varphi_S) + RT_3 K_{81}(\theta_S,\varphi_S)\}, \quad (47)$$

respectively.

For a symmetric linear molecule the first coupling term comes from the product

$$\sum_{uvnr} {}_{22uv}A^2_{nrmp}\, y_{2uv}(\theta_S,\varphi_S)\, y_{2nr}(\theta_S,\varphi_S) = \beta_1 K_{01}(\theta_S,\varphi_S) + \beta_2 K_{41}(\theta_S,\varphi_S), \quad (48)$$

where β_1 and β_2 are different linear combinations of the five possible coefficients ${}_{22uv}A^2_{nrmp}$. In the structure factor the corresponding term is

$$\exp(-\tfrac{1}{2}b^2_{xy} S^2)(b_{xy} S)^2\{g_x j_2(2\pi S r_1) + g_y j_2(2\pi S r_2)\} \times \{RT_1 K_{01}(\theta_S,\varphi_S) + RT_2 K_{41}(\theta_S,\varphi_S)\}. \quad (49)$$

Compared to (46)–(47) this term is quadratic in the center-of-mass displacements, because of higher molecular symmetry. In the following, radial parts of these model functions are used to explain curves $F_{lnr}(S)$ obtained by direct multipole analysis.

KCN, NaCN, KOD *and* NaOD. Neutron diffraction data from KCN (Rowe, Hinks, Price & Susman, 1973), NaCN (Rowe *et al.*, 1973), KOD (Kabs, 1980) and NaOD (Bleif, 1978) were first treated by direct multipole analysis. Direct multipole analysis calculates deviations of $f(\omega,\mathbf{R})$ from a given sphere within a sphere with radius half of the distance between the neighboring ions. The parameters of the given sphere, bond lengths and mean-square amplitudes, were taken from a separate fit (Table 1). The resulting curves of the direct multipole analysis are the solid lines in Figs. 1–4. To these curves radial parts of the model functions (41), (43), (46) and (47) were then fitted within each multipole order separately.

For KCN the experimental data indicate significant deviations from the spherical-ion reference model in the zeroth-, fourth- and sixth-order multipole components. The zeroth-order term $\Delta F_{01}(S)$ is well explained with the model curve (43*a*), indicating isotropic anharmonicity in the center-of-mass motion of the dipole. But $\Delta F_{01}(S)$ is also very sensitive to several other effects, including extinction and thermal diffuse scattering. Therefore, the numerical value of the parameter τ_{401}, given in Table 1, should be taken rather as an indication of the phenomenon than as an exact measure of it.

Table 1. *Final values of parameters for* KCN, KOD, NaCN *and* NaOD *from direct multipole analysis*

	KCN	KOD	NaCN	NaOD
Bond length (Å)	0·650 (5)$_C$	0·12 (2)$_O$	0·65 (1)$_C$	0·10 (2)$_O$
	+0·550 (5)$_N$	+0·98 (2)$_D$	+0·55 (1)$_N$	+0·82 (2)$_D$
$\langle u_M^2\rangle$ (Å^2)	0·061 (1)	0·120 (5)	0·070 (2)	0·154 (6)
$\langle u_{XY}^2\rangle$ (Å^2)	0·057 (1)	0·080 (3)	0·060 (2)	0·086 (3)
τ_{401}	0·038 (5)	–	0·035 (8)	–
τ_{441}	−0·053 (3)	–	0·049 (3)	–
τ_{661}	0·035 (1)	–	–	–
R_4	−0·078 (6)	−0·21 (2)	0·110 (6)	−0·23 (3)
R_6	0·384 (8)	−0·15 (2)	–	−0·12 (11)
R_8	−0·14 (7)	0·58 (5)	0·23 (9)	–

$$f(\theta,\varphi) = 1/4\pi + \textstyle\sum_l R_l K_{l1}(\theta,\varphi)$$

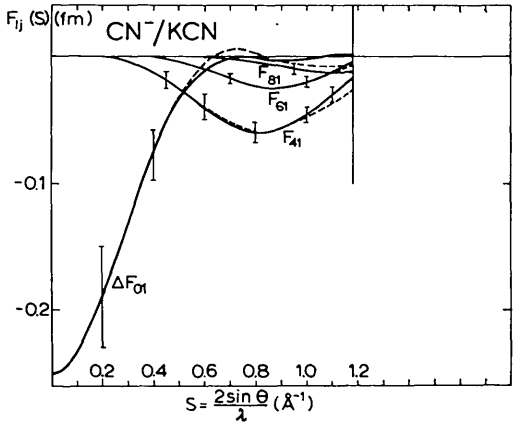

Fig. 1. Radial scattering amplitudes for CN^- in KCN. The solid lines are calculated by direct multipole analysis with a spherical reference model (see text). The error bars refer to the statistical errors of the experimental structure factors. The vertical line at $S = 1{\cdot}18$ (Å^{-1}) shows the cut-off of the measured reflections. Model curves (broken lines) are calculated from equations (41), (43*a*) and (43*b*) with parameters given in Table 1.

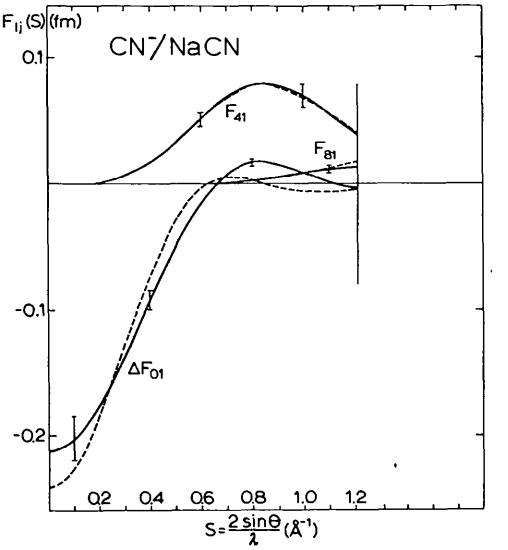

Fig. 2. Radial scattering amplitudes for CN^- in NaCN. The solid lines are calculated by direct multipole analysis with a spherical reference model (see text). The error bars refer to the statistical errors of the experimental structure factors. The vertical line at $S = 1{\cdot}21$ (Å^{-1}) shows the cut-off of the measured reflections. Model curves (broken lines) are calculated from equations (41), (43*a*) and (43*b*) with parameters given in Table 1.

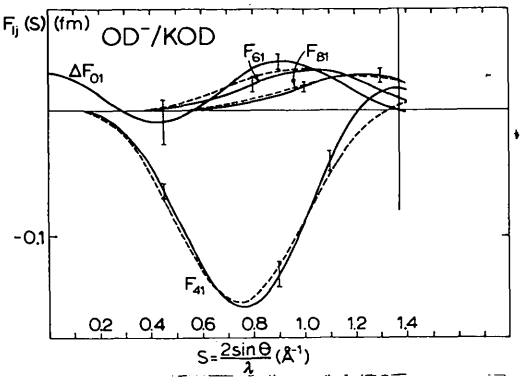

Fig. 3. Radial scattering amplitudes for OD^- in KOD. The solid lines are calculated by direct multipole analysis with a spherical reference model (see text). The error bars refer to the statistical errors of the experimental structure factors. The vertical line at $S = 1{\cdot}37$ (Å^{-1}) shows the cut-off of the measured reflections. Theoretical curves (broken lines) are calculated from equation (41) with parameters given in Table 1.

Model curves (43*b*) and (41) with parameter values $\tau_{441} = -0{\cdot}053$ and $R_4 = -0{\cdot}08$ explain very well the fourth-order term. The sixth-order term $F_{61}(S)$ is very well explained with model curves (43*c*) and (41) and parameter values $\tau_{661} = -0{\cdot}035$ and $R_6 = 0{\cdot}38$. Since R_4 is negative and R_6 positive and larger, the orientational probability distribution of the CN^- ion has maxima in the [111] and symmetry-related directions and minima in the [110] and related directions. The maxima and minima of the translational probability distribution are in the same directions, but smaller. A small and negative eighth-order component, $R_8 = -0{\cdot}14$, would indicate slight local minima in the [100] and related directions for the orientational probability distribution.

Although both the orientational and translational probability distributions are anisotropic and $f(\theta,\varphi)$ is slightly negative in the [110] and related directions, it was not possible to separate the coupling terms (46) and (47) from $F_{41}(S)$ and $F_{61}(S)$, respectively. For K^+ the solid line $F_{41}(S)$ was positive and exceeded the limits of error by a factor of four. If this is real, it indicates a slightly larger probability of vibrations in the [100] and related directions. In the analysis the bond-length parameters r_C and r_N remained the same as in the separate fit. Compared to the results of Rowe *et al.* (1973) R_4 is now smaller, R_6 larger and, in addition, R_8 is now determined, although somewhat inaccurately.

The results for NaCN are not consistent with the corresponding results for KCN. The zeroth-order terms $\Delta F_{01}(S)$ for CN^- and Na^+ are large and could not be well explained by any of the present model curves. It is therefore concluded that the data are not free from extinction, thermal diffuse scattering or other corrections of an isotropic nature.

For KOD the orientational probability distribution of OD^- has maxima in the [111] and symmetry-related directions and minima in the [100] and related directions; there are in addition small local minima in the [110] and related directions. If $R_6 = -0{\cdot}15$ and $R_8 = 0{\cdot}58$ are included as significant parameters, the orientational probability distribution would have maxima in the [110], minima in the [113] and local maxima in the [100] and symmetry-related directions.

Although $f(\theta,\varphi)$ with $R_4 = -0{\cdot}21$ is slightly negative in the [100] and related directions, it was not possible to separate the center-of-mass anharmonicity term (43) and the coupling term (46) from the solid line $F_{41}(S)$.

In KOD the solid lines for K^+ did not show any significant deviations from the spherical-ion reference model. A fit gave the value $R_4 = -0{\cdot}35$ (4) ($R_w = 3{\cdot}5\%$) for the orientational parameter, which is slightly larger than the result of this analysis.

For NaOD the results are consistent with the corresponding ones for KOD. Since $R_6 \simeq 0$ and $R_8 = 0$ the orientational motion of the OD^- dipole is slightly stronger in NaOD than in KOD. For Na^+ the solid line $F_{41}(S)$ exceeded the limits of error by a factor of five. A fit gave the value $R_4 = -0{\cdot}36$ (3) ($R_w = 3{\cdot}6\%$) for the orientational parameter in NaOD, which is slightly larger than the present value. Present results for the orientational probability distribution of the OD^- dipole agree with those of Bleif (1978), obtained by the Fourier-synthesis method.

Conclusion. In orientationally disordered molecular crystals where a small linear ion is at a cubic *m*3*m* site orientation–translation coupling is small. In the present examples the main uncertainty in the calculated parameters comes from the thermal diffuse scattering.

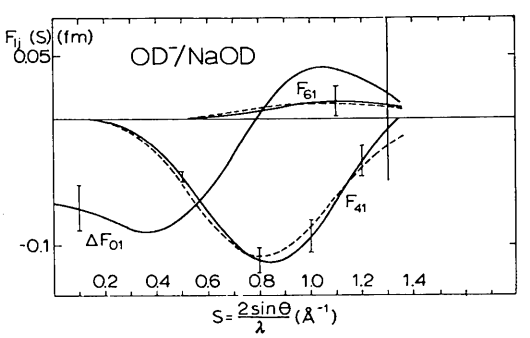

Fig. 4. Radial scattering amplitudes for OD^- in NaOD. The solid lines are calculated by direct multipole analysis with a spherical reference model (see text). The error bars refer to the statistical errors of the experimental structure factors. The vertical line at $S = 1{\cdot}30$ (Å^{-1}) shows the cut-off of the measured reflections. Model curves (broken lines) are calculated from equation (41) with parameters given in Table 1.

Tetrahedral body at a cubic m3m site

A tetrahedral molecule or ion at a cubic *m*3*m* site is another example of a common structure among orientationally disordered molecular crystals. The static radial form factors are now

$$g_{lj}(S) = 4\pi i^l\, 4g_x\, K_{lj}(111)\, j_l(2\pi S r_0),\ l = 3, 4, 6, 7, 8, 10, \tag{50}$$

up to $l = 10$. In the structure factor lowest-order terms deriving their origin from the uncorrelated probability distribution are

$$R_l\, i^l \exp(-\tfrac{1}{2}b^2 S^2)\, g_x j_l(2\pi S r_0)\, K_{l1}(\theta_S,\varphi_S),\quad l = 4, 6, 8, 10, \tag{51}$$

where $b = 2\pi\langle u^2\rangle^{1/2}$ and $R_l = (8\pi^2/2l + 1)\, 4\pi K_{l1}(111)\, a^l_{11}$. The a^l_{11} are expansion coefficients of $f(\omega)$ in the cubic rotator basis:

$$f(\omega) = \sum_l a^l_{11}\, C^l_{11}(\omega). \tag{52}$$

Lowest-order terms deriving their origin from the anharmonic translational probability distribution are

$$B_1 \exp(-\tfrac{1}{2}b^2 S^2)\{\tfrac{15}{8} - \tfrac{5}{2}b^2 S^2 + \tfrac{1}{2}b^4 S^4\} \times \{g_y + 4g_x j_0(2\pi S r_0)\} K_{01}(\theta_S,\varphi_S), \quad (53a)$$

$$B_2 \exp(-\tfrac{1}{2}b^2 S^2)\, b^4 S^4 \{g_y + 4g_x j_0(2\pi S r_0)\} K_{41}(\theta_S,\varphi_S) \quad (53b)$$

$$B_3 \exp(-\tfrac{1}{2}b^2 S^2)\, b^6 S^6 \{g_y + 4g_x j_0(2\pi S r_0)\} K_{61}(\theta_S,\varphi_S), \quad (53c)$$

where $B_1 = \tau_{401}\pi\sqrt{2}(\langle u^2\rangle^{1/2})^3$, $B_2 = \tau_{441}\pi\sqrt{2}(\langle u^2\rangle^{1/2})^3$ and $B_3 = -\tau_{661}\pi\sqrt{2}(\langle u^2\rangle^{1/2})^3$. The first coupling terms are the same as for a linear ion at a cubic ($m3m$) site:

$$RT_1 \exp(-\tfrac{1}{2}b^2 S^2)\, bS\, 4g_x j_3(2\pi S r_0) K_{41}[\theta_S,\varphi_S), \quad (54)$$

$$RT_2 \exp(-\tfrac{1}{2}b^2 S^2)\, bS\, 4g_x j_7(2\pi S r_0) K_{61}(\theta_S,\varphi_S), \quad (55)$$

$$RT_3 \exp(-\tfrac{1}{2}b^2 S^2)\, bS\, 4g_x j_7(2\pi S r_0) K_{81}(\theta_S,\varphi_S), \quad (56)$$

where RT_1, RT_2 and RT_3 are again different linear combinations of the multipole expansion coefficients of $f(\omega,\mathbf{R})$.

The first quadratic coupling term, $h = t = 2$, in the center-of-mass displacements comes from the product

$$\sum_{uvnr} {}_{22uv}A^4_{nrl}\, y_{2uv}(\theta_S,\varphi_S)\, y_{4nr}(\theta_S,\varphi_S) = \beta_1 K_{41}(\theta_S,\varphi_S) + \beta_2 K_{61}(\theta_S,\varphi_S). \quad (57)$$

In the structure factor the corresponding terms are

$$RT_4 \exp(-\tfrac{1}{2}b^2 S^2)\, b^2 S^2\, 4g_x j_4(2\pi S r_0) K_{41}(\theta_S,\varphi_S), \quad (58)$$

$$RT_5 \exp(-\tfrac{1}{2}b^2 S^2)\, b^2 S^2\, 4g_x j_4(2\pi S r_0) K_{61}(\theta_S,\varphi_S). \quad (59)$$

In the following, results from direct multipole analysis are explained by the radial parts of these model functions.

CBr_4. The solid lines in Fig. 5 are results from direct multipole analysis of the neutron diffraction data of More, Lefebvre, Hennions, Powell & Zeyen (1980). Reflexions with $F^{obs} = 0$ have been omitted, since they are not informative in direct multipole analysis. Reflexions 200 and 111 were omitted because of extinction. Inclusion of these reflexions would make the zeroth- and fourth-order terms $\Delta F_{01}(S)$ and $F_{41}(S)$ slightly larger.

It is obvious from the results that the experimental data indicate significant deviations from the spherical-ion reference model only in the fourth- and sixth-order multipole components. Model curves (53) and (54) together, with parameter values $\tau_{441} = -0{\cdot}003$ and $RT_1 = 0{\cdot}12$, explain very well the fourth-order component $F_{41}(S)$. Since τ_{441} is negative the center-of-mass vibrations have slightly larger probability in the [100] and symmetry-related directions. The presence of the RT_1 term indicates that in these directions the center-of-mass motion is coupled to rotations of the molecule. Probably through this coupling the molecule avoids the sterically impossible [111] orientation. Inclusion of the fourth-order orientational term (51) did not improve the present explanation of the observed $F_{41}(S)$ term.

The sixth-order component $F_{61}(S)$ is rather well explained by the model curve (51) alone, with parameter $a^6_{11} = -0{\cdot}00167$. The small difference between the maximum of the model curve and the solid line would indicate a small change in the bond length. The explanation of the fourth-order component does not, however, support this. Since a^6_{11} is negative, the orientational probability distribution has maxima in the [110] and minima in the [111] and symmetry-related directions. With respect to the positivity condition of $f(\omega)$, the absolute value of a^6_{11} is large, but does not indicate orientation–translation correlations; it may indicate intermolecular angular correlations. Since the molecule is rather large, oscillations of the zeroth-order term may now also indicate non-rigidity of the molecule.

Compared to the results of Press *et al.* (1979) and More *et al.* (1980) a^4_{11} and a^8_{11} are now zero, within the limits of the statistical accuracy of the data. The first difference comes from the center-of-mass anharmonicity, the second difference is obvious. The absolute value of the sixth-order orientational parameter is now

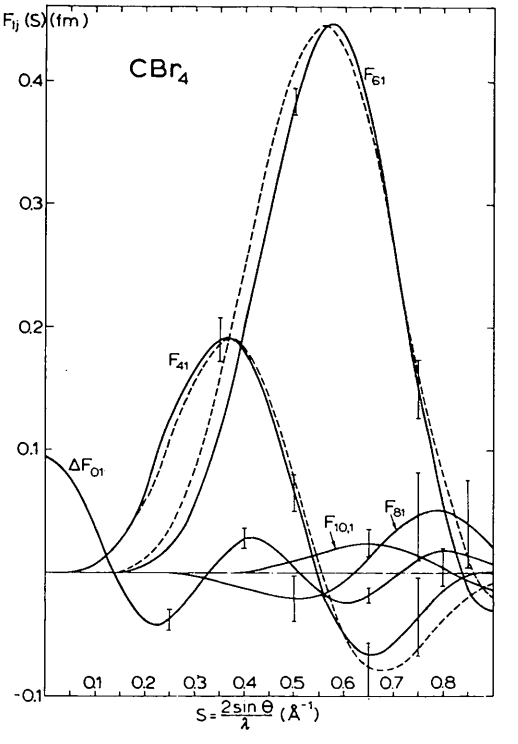

Fig. 5. Radial scattering amplitudes for CBr_4. The solid lines are calculated by direct multipole analysis with a spherical reference model (see text). The error bars refer to the statistical errors of the experimental structure factors. The cut-off value of the measured reflections is $S = 0{\cdot}90$ (Å^{-1}). Theoretical curves (broken lines) are calculated from equations (51), (54) and (53*b*) with parameters given in Table 2.

larger than was reported in these two works. Press *et al.* (1979) included also orientation–translation correlations. Their value for RT_1 agrees, within the limits of error, with the present value.

NH_4Cl *and* ND_4NO_3. Direct multipole analysis results for NH_4Cl (Kurki-Suonio, Merisalo, Vahvaselkä & Larsen, 1976) and for ND_4NO_3 (Ahtee *et al.*, 1979) are given in Table 2 for comparison. Clearly the corresponding model curves cannot be improved by including the center-of-mass anharmonicity and coupling. For CBr_4, NH_4^+ and ND_4^+ and libration amplitude was estimated using the formulas given by Ahtee *et al.* (1979). The a^l_{11} values for CBr_4 and NH_4^+ are not consistent with one libration amplitude. Therefore the $\langle\theta^2\rangle^{1/2}$ given for them is only a rough estimate.

Planar triangular ion at $\bar{3}m$ *site*

The static radial form factors of a rigid planar triangle $\bar{6}m2$ are

$$g_{lmp}(S) = 4\pi i^l\, 3g_x\, y_{lmp}(h_0\, k_0\, l_0)\, j_l(2\pi S r_0),$$
$$lmp = (l + 2j, 3\mu, +) \qquad (60)$$

In the structure factor, lowest-order terms deriving their origin from the anisotropic translational probability distribution of the triangle are

$$B_1 \exp(-\tfrac{1}{2}b^2 S^2)\{\tfrac{3}{2} - b^2 S^2\}\{g_y + 3g_x j_0(2\pi S r_o)\} \times y_{00+}(\theta_S,\varphi_S), \qquad (61a)$$

$$B_2 \exp(-\tfrac{1}{2}b^2 S^2)\, b^2 S^2\{g_y + 3g_x j_0(2\pi S r_0)\}\, y_{20+}(\theta_S,\varphi_S), \qquad (61b)$$

$$B_3 \exp(-\tfrac{1}{2}b^2 S^2)\, b^4 S^4\{g_y + 3g_x j_0(2\pi S r_0)\}\, y_{43+}(\theta_S,\varphi_S), \qquad (61c)$$

where $b = 2\pi\langle u^2\rangle^{1/2}$, $B_1 = -\tau_{200+}\,\pi\sqrt{2}(\langle u^2\rangle^{1/2})^3$, $B_2 = -\tau_{220+}\,\pi\sqrt{2}(\langle u^2\rangle^{1/2})^3$, $B_3 = \tau_{443+}\,\pi\sqrt{2}(\langle u^2\rangle^{1/2})^3$. Terms deriving their origin from the uncorrelated probability distribution of the triangle are

Table 2. *Final values of parameters for* CBr_4 *and corresponding results for* NH_4Cl *(Kurki-Suonio et al., 1976) and for* ND_4NO_3 *(Ahtee et al., 1979) from direct multipole analysis*

	CBr_4	NH_4^+	ND_4^+	NO_3^-
Bond length (Å)	1·92 (1)	1·050 (5)	0·99 (1)	1·23 (1)
$\langle u^2\rangle$ (Å^2)	0·185 (2)	0·025 (1)	0·146 (1)	0·181 (1)
τ_{441}	−0·0010 (3)	–	–	–
a^4_{11}	–	−0·00286 (6)	−0·0028 (5)	−0·0048 (5)
a^6_{11}	−0·00167 (8)	−0·00250 (8)	0·001 (2)	0·002 (2)
a^8_{11}	–	0·0041 (3)	0·0003 (3)	0·0004 (4)
a^{10}_{11}	−0·0005 (4)	−0·0027 (4)	–	–
RT_1	0·12 (2)	–	–	–
RT_2	0·006 (5)	–	–	–
$\langle\theta^2\rangle^{1/2}$ (°)	16 (2) (from a^6_{11})	7 (2) (from a^{10}_{11})	22 (2) (from a^4_{11})	–

$f(\omega) = \sum_l a^l_{11}\, C^l_{11}(\omega)$.

$$R_{lnr} \exp(-\tfrac{1}{2}b^2 S^2)\, 3g_x j_l(2\pi S r_0)\, y_{lnr}(\theta_S,\varphi_S), \qquad (62)$$

where

$$R_{lnr} = (32\pi^3/2l + 1)\, i^l \sum_{mp} y_{lmp}(h_0\, k_0\, l_0)\, a^l_{nrmp}. \qquad (63)$$

a^l_{nrmp} are expansion coefficients of $f(\omega)$ in the non-cubic-site – non-cubic-body rotator basis (*cf.* I)

$$f(\omega) = \sum_{lnrmp} a^l_{nrmp}\, C^l_{nrmp}(\omega). \qquad (64)$$

Because of the low body symmetry only the a^2_{0+0+}, a^4_{0+0+} and a^4_{3+0+} terms can be solved numerically from the R_{lnr} values.

The first coupling term comes from the product

$$\sum_{unvr} {}_{11uv}A^i_{nr0+}\, y_{1uv}(\theta_S,\varphi_S)\, y_{1nr}(\theta_S,\varphi_S) = \alpha_1\, y_{00+}(\theta_S,\varphi_S) + \alpha_2\, y_{20+}(\theta_S,\varphi_S), \qquad (65)$$

where α_1 and α_2 are different linear combinations of the three possible ${}_{11uv}A^l_{nr0+}$ coefficients. In the structure factor the corresponding terms are

$$RT_1 \exp(-\tfrac{1}{2}b^2 S^2)\, bS\, 3g_x j_1(2\pi S r_0)\, y_{00+}(\theta_S,\varphi_S) \qquad (66)$$

$$RT_2 \exp(-\tfrac{1}{2}b^2 S^3)\, bS\, 3g_x j_1(2\pi S r_0)\, y_{20+}(\theta_S,\varphi_S). \qquad (67)$$

In the following, radial parts of these model functions are used to explain the solid lines of Fig. 6 obtained by direct multipole analysis.

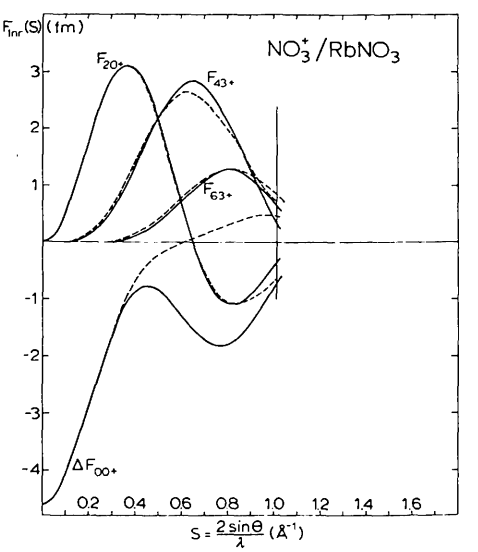

Fig. 6. Radial scattering amplitudes for NO_3^+ in $RbNO_3$. The solid lines are calculated by direct multipole analysis with a spherical reference model (see text). The error bars are of the order of the line width. The vertical line at $S = 1{\cdot}10$ (Å^{-1}) shows the cut-off of the measured reflections. Theoretical curves (broken lines) are calculated from equations (61*a*), (61*b*), (62) and (67) with parameters given in Table 3. The curves are drawn with max $\{y_{lnr}\} = 1$ normalization.

Table 3. *Final values of parameters for* $RbNO_3$ *from direction multipole analysis*

	NO_3^-		NO_3^-		NO_3^-
Bond length (Å)	1·24 (1)	a^2_{0+0+}	0·0060 (2)	R_{60+}	−1·73 (2)
		a^0_{0+0+}	0·0080 (1)	R_{63+}	0·015 (1)
$\langle u^2\rangle$ (Å²)	0·101 (1)	a^3_{3+0+}	−0·00224 (1)	R_{66+}	−0·0002 (1)
τ_{200+}	0·224			RT_1	–
τ_{220+}	0·358 (28)			RT_2	0·15 (1)
τ_{443+}	0·0053 (4)				

$$f(\omega) = \sum_{lmpnr} a^l_{mpnr}\, C^l_{mpnr}(\omega),$$
where $R_{lmp} = (32\pi^3/2l+1)\, i^l \sum_{nr} y_{lnr}(100)\, a^l_{mpnr}$.

$RbNO_3$. Neutron diffraction data from rhombohedral $RbNO_3$ has been analyzed by Ahtee, Kurki-Suonio & Vahvaselkä (1981). The four most significant terms of their direct multipole analysis, with a spherical-ion reference model, are given in Fig. 6. Parameter values are given in Table 3.

Model curve (61*a*) with $\tau_{200+} = 0{\cdot}224$ explains the zeroth-order term only up to $S = 0{\cdot}35$ (Å^{-1}). Inclusion of the coupling term does not improve the fit. It is probable that this large zeroth-order term is a consequence of thermal diffuse scattering.

Model curves (61*b*), (62) and (67) with parameters $\tau_{220+} = 0{\cdot}358$, $R_{20+} = 0{\cdot}37$ and $RT_2 = 0{\cdot}15$ explain very well the second-order term. The τ_{220+} term indicates that the center-of-mass vibrations are anisotropic, with the principal axis of the thermal ellipsoid along the z axis. The presence of R_{20+} and RT_2 terms together with τ_{220+} shows that librations of the triangle depend on its position along the z axis.

The fourth-order term $F_{43+}(S)$ is very well explained by model curves (62) and (61*c*) with parameters $R_{43+} = 0{\cdot}067$ and $\tau_{443+} = 0{\cdot}005$, respectively. The term τ_{443+} indicates that the center-of-mass vibrations are slightly anisotropic also in the xy plane.

All other solid lines are explainable by model curves (62) and related orientational parameters.

Compared to the results of Ahtee *et al.* (1981) the present analysis gives more detailed information about the time-averaged thermal behavior of the NO_3^- ion. In particular, orientational parameters are now separated from those describing translations and from those describing coupling between these two. The main new information comes from the observed coupling and related anisotropy of vibrations.

6. Discussion and conclusions

This work differs in three aspects from the work of Press *et al.* (1979), where rotation–translation coupling was studied for orientationally disordered molecules at cubic sites. Firstly, here coupling is treated for all body and site symmetries. Secondly, center-of-mass anharmonicities are here included. And thirdly, and most importantly, the present method, symmetrized multipole formalism, is formulated for use with direct multipole analysis. Since the number of parameters, in the presence of coupling and anharmonicities, is large, the last difference is of crucial importance. In a normal fit there are more than ten parameters and they are strongly correlated. For example, in NaOD R_4 and RT_1 were correlated with element −0·98 in the normalized correlation matrix. With 18 data points the resulting $R_w = 2{\cdot}9\%$ is not significantly better, at the 0·005 level (Hamilton, 1965), than $R_w = 3{\cdot}6\%$ found without the RT_1 term. A normal fit was also tried in the other examples with similar difficulties.

In the direct multipole analysis we only need to explain the radial scattering amplitudes within each multipole order separately; and there the number of parameters, even in the presence of coupling and vibrational anisotropy, is seldom larger than four. In the direct multipole analysis we are thus interested in the relationship between the radial multipole coefficients of the static and dynamic form factors. In the symmetrized multipole formalism the multipole expansion coefficients of the total rigid body distribution $f(\omega,\mathbf{R})$ are parameters mediating this relationship. In favourable cases it is a simple relation between radial terms of the same multipole order. In the uncorrelated situation this is the case for nearly angle-independent distribution $f(\omega)$ and for nearly isotropic translational probability distribution $\tau(\mathbf{R})$. In the presence of coupling, and for vibrational anisotropy, the multipole order between these radial terms is mixed. Because of this the multipole expansion coefficients of the correlated part of $f(\omega,\mathbf{R})$ are not separable. Coupling affects the radial behaviour of the scattering factors in some multipole orders, and this can be observed by the present method, but this information cannot be transferred or packed in the probability distribution.

For the convergence of the correlated part of the dynamic structure factor both high body and high site symmetry are important for two reasons. Firstly, the order of the spherical Bessel functions entering into the form factor, which come from the Fourier transform of the static density, is high for high body symmetries. Secondly, the number of different coupling terms in the structure factor is low for high site symmetries. Moreover, the coupling term in the structure factor is proportional to an exponent of the mean-square amplitude and this exponent is one for low body symmetries.

One can thus expect, *a priori*, that coupling is important in orientationally disordered molecular crystals with low site and low body symmetries where the mean-square amplitude of the center-of-mass motion is large. But, naturally, the ultimate significance of coupling is determined by the actual physical situation.

In the present examples coupling was observed only in CBr_4 and $RbNO_3$. It seems that the main remaining uncertainty, in the examples, comes from the thermal diffuse scattering. It certainly has some effect on the values of the present parameters, at least for isotropic ones.

Clearly, the next step forward, in the interpretation of molecular motion in orientationally disordered crystals, would be the study of the effect of intermolecular orientational correlations.

I would like to thank Dr M. Kabs from the Hahn–Meitner Institut for providing me with his neutron diffraction data from KOD prior to publication. Financial support from the Project Neutron Scattering IIKW, Belgium and Emil Aaltonen Foundation, Finland is gratefully acknowledged.

APPENDIX

Site-symmetric coupling term

The correlated part of $F(\mathbf{S})$ is

$$\sum_{uvnr} {}_{htuv}A^{l}_{nrmp}\, y_{tuv}(\theta_S,\varphi_S)\, y_{lnr}(\theta_S,\varphi_S), \qquad (A1)$$

where $l \neq 0$ or $t \neq 0$. Indices t and l determine the order of magnitude of the coupling term. For $t = 1$ orientations are coupled to center-of-mass displacements linear in R, for $t = 2$ quadratically *via* R^2, and so on. Index l, determined by the body symmetry, determines the spherical Bessel function entering into the coupling term through $g_{lmp}(S)$.

From the coupling rule for the spherical harmonic, with Clebsch–Gordon coefficients as determined by Rose (1957, §10), the product term ($A1$) can be written

$$\sum_{uvnr} {}_{htuv}A^{l}_{nrmps}[(2t+1)(2l+1)/8\pi(2s+1)$$
$$\times (1+\delta_{u0})(1+\delta_{n0})]^{1/2}$$
$$\times c(tls;00)\, p[(1+\delta_{u+n,0})^{1/2}\, c(tls;un)\, y_{s,u+n,vr}(\theta_S,\varphi_S)$$
$$+ r(-1)^n(1+\delta_{u-n,0})^{1/2}\, c(tls;u-n)\, y_{s,u-n,vr}(\theta_S,\varphi_S)],$$

where $p = -1$ for $v = r = -$, otherwise $p = +1$, $|t-l| \leq s \leq t+l$ and $t+l+s =$ even. The last parity rule follows from the fact that $c(tls;00) \neq 0$ only for $t+l+s =$ even.

Now the coupling term, and the corresponding part of $f(\omega,\mathbf{R})$, is site symmetric when the site-symmetric-index picking rules are applied to $y_{s,u+n,vr}$ and to $y_{s,u-n,vr}$, within the parity rule.

For cubic site symmetries, the real spherical harmonics combine further to cubic harmonics (*cf.* I).

References

AHTEE, M., KURKI-SUONIO, K., LUCAS, B. W. & HEWAT, A. W. (1979). *Acta Cryst.* A**35**, 591–597.

AHTEE, M., KURKI-SUONIO, K. & VAHVASELKÄ, A. (1981). In preparation.

BLEIF, H. J. (1978). Thesis. Univ. of Tübingen.

HAMILTON, W. C. (1965). *Acta Cryst.* **18**, 502–510.

KABS, M. (1980). Personal communication.

KARA, M. & KURKI-SUONIO, K. (1981). *Acta Cryst.* A**37**, 201–210.

KURKI-SUONIO, K., MERISALO, M. & PELTONEN, H. (1979). *Phys. Scr.* **19**, 57–63.

KURKI-SUONIO, K., MERISALO, M., VAHVASELKÄ, A. & LARSEN, F. K. (1976). *Acta Cryst.* A**32**, 110–115.

MORE, M., LEFEBVRE, J., HENNIONS, B., POWELL, B. M. & ZEYEN, C. M. E. (1980). *J. Phys. C*, **13**, 2833–2846.

PRESS, W., GRIMM, H. & HÜLLER, A. (1979). *Acta Cryst.* A**35**, 881–885.

ROSE, M. E. (1957). *Elementary Theory of Angular Momentum*. New York: Wiley.

ROWE, J. M., HINKS, D. G., PRICE, D. L. & SUSMAN, S. (1973). *J. Chem. Phys.* **58**, 2039–2042.

SCHOMAKER, V. & TRUEBLOOD, K. N. (1968). *Acta Cryst.* B**24**, 63–76.

WILLIS, B. T. M. & PRYOR, A. W. (1975). *Thermal Vibrations in Crystallography*. Cambridge Univ. Press.